DIAGNOSTYKA, 2022, Vol. 23, No. 4

e-ISSN 2449-5220
DOI: 10.29354/diag/156382

STRUCTURAL DIAGRAM OF THE BUILT-IN DIAGNOSTIC SYSTEM FOR ELECTRIC DRIVES OF VEHICLES

Oleg GUBAREVYCH [1,*], Sergey GOOLAK [1], Inna MELKONOVA [2], Mariia YURCHENKO [3]

[1] Department of Electromechanics and Rolling Stock of Railways, State University of Infrastructure and Technologies (04071), Ukraine
[2] Department of Electrical Engineering, Volodymyr Dahl East Ukrainian National University, (93400), Ukraine
[3] Faculty of Management and Technology, State University of Infrastructure and Technologies (04071), Ukraine
[*]Corresponding author, e-mail: oleg.gbr@ukr.net

Abstract

Currently, in transport systems, as part of the main and auxiliary equipment, a large number of induction motors with a squirrel-cage rotor of different capacities are used. Their wide application in the transport industry is associated with the main advantages over other types of machines – a fairly high reliability, low cost and ease of maintenance. However, during the operation of these motors, a number of malfunctions can occur that affect the deterioration of the performance of the entire drive, the accuracy of its functions, or accelerate an emergency stop. To ensure proper control of the technical condition of electric motors, modern diagnostic systems are required that operate in real-time and operational loading mode with the transmission of data on the instantaneous state of the main control elements. The paper proposes a block diagram of the diagnostic built-in system and developed a modular unit for it to set the type and degree of the most complex damage – inter-turn short circuit in the stator winding.

Keywords: diagnostic system; induction electric motor; inter-turn short circuit; stator defect

1. INTRODUCTION

Improving the efficiency of transport vehicles, especially the main types of rail, water and air transport, proportionally contributes to the development of other industries in each country. To ensure the efficiency of the operation of the transport infrastructure, the most important issues are to improve the operational reliability of equipment and the safety of transportation.

Therefore, the main characteristic of each equipment is its reliability, which requires constant monitoring of the appearance and development of defects with obtaining information about them sufficient to predict the time of trouble-free operation during operation. Timely detection of damage to equipment elements with the adoption of measures to eliminate them or their planned replacement leads to the prevention of emergency failures with subsequent economic damage. Most of the failures of transport equipment occur in electric drives of various mechanisms and devices, where the main element is the electric motor [1, 2].

Currently, in transport systems, as part of the main and auxiliary equipment, a large number of induction motors with a squirrel-cage rotor of different capacities are used. Their wide application in the transport industry is associated with the main advantages over other types of machines – a fairly high reliability, low cost and ease of maintenance. However, during the operation of these motors, a number of malfunctions may occur [3-5]. These faults can affect the performance of the drive, the accuracy of its functions, or accelerate the failure of the motor in emergency mode.

The main condition contributing to the reduction of failures during the operation period is the timely diagnosis and prediction of the current state of electric motors.

The relevance of the problem of assessing the current operational reliability of transport electric motors and their components is due to the fact that a significant part of them are operated in fairly harsh conditions with a high failure cost. The peculiarity of their operation for various types of transport lies in the complex effect of a number of complex factors, such as the rapidly changing nature of work loads, vibromechanical loads, including those from working mechanisms, high and low temperatures, significant pressure drops, high humidity, etc.

Proper monitoring of the technical condition of electric motors can only be provided by diagnostic systems built into the electric drive that operate in real time and operational loading mode with the transmission of data on the instantaneous state of the main control elements. In addition, a modern and efficient diagnostic system should allow obtaining information not only about the output of some operating parameters beyond the established limits, but also to differentiate the type of malfunction and the degree of damage. Reliable installation of the type and degree of damage to the electric motor makes it possible to increase the accuracy of predicting the period of its failure-free operation and thereby ensure the planning of time for their elimination.

2. THE AIM AND OBJECTIVES OF RESEARCH

The aim of research is to develop a block for setting the type and degree of damage to the winding stator as part of the proposed block diagram of the built-in diagnostic system for monitoring the state of an induction motor. This will make it possible to more accurately determine the type and degree of damage to the winding stator as part of the diagnostic system of transport equipment during the operation of induction motors when predicting no-failure operation.

To achieve the aim, the following objectives were set:

- to analyze the damageability of induction electric motors with a squirrel-cage rotor;
- determine nodes and types of damage for ongoing monitoring;
- to develop a block diagram built into the drive system for diagnosing induction electric motors;
- to develop an algorithm for the operation of the module for monitoring the presence of inter-turn short circuits in the stator winding;
- to develop a block diagram of the block of the diagnostic system to identify the degree of inter-turn short circuit in the stator winding under static and dynamic loads of the electric motor in the presence of an asymmetric power supply system.

3. DEVELOPMENT OF THE STRUCTURAL DIAGRAM OF THE DIAGNOSTICS SYSTEM BUILT-IN TO THE COMPOSITION OF THE DRIVE

To develop a block diagram of the system for diagnosing induction electric motors, an analysis of damage to nodes and defects was carried out. According to various data of operational statistics, taking into account the area of operation of induction motors with a squirrel-cage rotor, possible failures by the nodes of electric motors are distributed as follows [1, 5, 6]:

- stator failure 77–85%;
- failure of the rotor 6–8%;
- failure of bearing units 8–14%.

From this it follows that an effective system for diagnosing induction motors should provide technical control of the state of all the listed units of electric motors.

When drawing up a structural diagram of a diagnostic system, it is advisable to take into account and determine those defects of each node that appear during operation and relate to parametric failures that need to be controlled to prevent a catastrophic failure, that is, an emergency stop.

From the possible defects of each node considered below, the most informative, from the point of view of the authors, damage was selected for monitoring by the diagnostic system [2, 5, 6].

Common stator damage includes:

- inter-turn short circuit in the stator winding;
- short circuit on the case;
- inter-phase short circuit;
- open circuits of inter-circuit connections;
- weakening of the pressing of the stator pack:
- general weakening of the fastening elements of the stator core;
- weakening of the pressing density of the outer sheets and steel packages;
- ellipse of the internal bore of the stator relative to the axis of rotation of the rotor;
- incorrect axial mounting of the active packages of the rotor and stator;
- stator eccentricity:
- manufacturing defect of the laminated stator steel package;
- a defect in the stator installation during the installation of an electrical machine (this defect may also occur due to the weakening of the foundation during operation).

Rotor damage:

- breakage or violation of contact in the rods or rings "squirrel cage";
- destruction of key connections;
- twisting (bending) of the shaft;
- eccentricity of the outer surface of the rotor relative to the axis of its rotation;
- weakening of the pressing of the entire package of steel of the rotor or only in the area of the teeth;
- unbalance of the rotor;
- unsatisfactory articulation of the output end of the shaft with the actuator (quality and defects of the couplings);
- unsatisfactory balancing of the machine fan impeller.

Damage to bearing assemblies:

- destruction of bearings;
- wear of the seating surfaces of bearing shields;

In works [1, 5, 6], a quantitative analysis of the causes of an emergency stop of induction motors with a squirrel-cage rotor was carried out. The results of the analysis in percentage terms are shown in Fig.1.

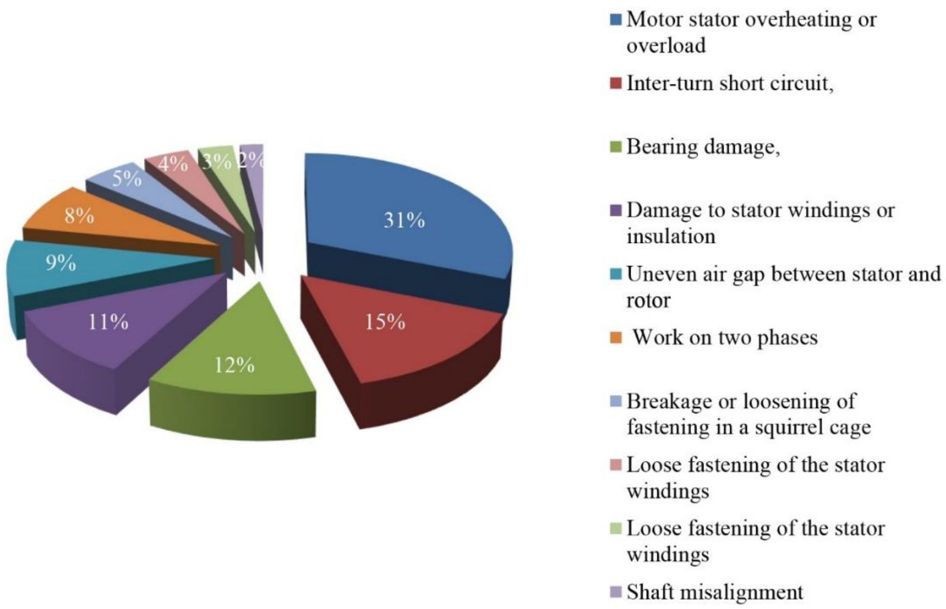

Fig. 1. The results of the analysis of the emergency stop of induction motors with a squirrel-cage rotor

Fig. 1 shows that the largest share of emergency stops of induction motors is due to overheating or overload of the motor (31%). These reasons relate to the violation of the operating conditions of the induction motor and are not considered in the system for diagnosing defects that have arisen in the induction motor [1, 3].

The next in terms of the number (15%) of the causes of failures is the occurrence of an inter-turn short circuit in the stator winding [3]. In the presence of this defect with a small number of short-circuited turns in the stator winding, the motor is in working condition [7-9]. In this case, the performance characteristics and energy indicators of the induction electric motor deteriorate [8, 9]. This defect is characterized by the fact that it can develop over time. When a certain number of short-circuited turns is reached, insulation breakdown occurs, as a result of which the electric motor fails. The ability to diagnose an inter-turn short circuit in the stator winding in the diagnostic system built into the drive is an urgent task.

Insulation damage (11%) caused by various factors is also not critical at the beginning of the defect. But in the process of developing a defect, it can also cause the electric motor to go out of working condition. This factor indicates the relevance of the presence in the diagnostic system built into the drive, the possibility of monitoring the state of the insulation [10, 11].

Damage to the bearings (12%) leads to the appearance of vibration and, over time, to the engagement of the rotor in the stator, resulting in damage to the rotor and stator with the closure of the active steel sheets of the magnetic circuit of these elements, which completely removes the electric motor from the working state [12-14]. Monitoring the condition of the bearings contributes to the timely detection of damage to the bearings and the prevention of an emergency stop of the electric motor. Therefore, the inclusion of bearing condition monitoring in the diagnostic system built into the drive is an urgent task.

Another defect that must be controlled during the operation of an electric motor as part of an electric drive is the control of the state of the rotor rods [15]. This defect is structurally included in the breakage or damage of the "squirrel cage" (5%) (Fig. 1). When melting or breaking the contact of one or two rods of a squirrel-cage rotor, the electric motor continues to be in working condition [16, 17]. However, when the motor is running with damaged rotor rods, the speed of rotation of the rotor with the same load will be less than in the same motor with a healthy rotor. In addition, a break or poor contact of the motor rotor rods is accompanied by vibration. In some cases, a motor with damaged rotor bars may not reach the operating rotor speed even with a light load. With a further increase in the number of damaged rods, the rotor of the loaded motor stops in emergency mode. In all cases, a motor with damaged rotor rods, operating under load, consumes increased current from the network and overheats more than a serviceable motor. To monitor the condition of the rotor, the study proposes to analyze the failure of double rods by monitoring the vibration signals in detail behind the three axes (-x, -y and -z) using an accelerometer. In [18], a new method for monitoring the state of the rotor, based on the analysis of the current of the stator line, is considered to improve the reliability of the emerging system for monitoring a defect in one rod of the rotor of an induction motor. This method combines the Electrical Time Synchronous Averaging (ETSA) procedure with the Vector Parking Transformation (VPT), Motor Current Signature Analysis (MCSA), and Fuzzy Logic Algorithm (FLA) method.

The unbalance of the rotating masses of an induction motor leads to vibration [19]. Regardless of the causes of occurrence, according to their external signs, the specifics of manifestation in the overall picture of vibration, all unbalances can be divided into two types – static unbalance and dynamic unbalance. Usually, the vibration pattern of unbalance appears simultaneously on two bearings of the controlled mechanism. Vibration from unbalance, in many cases, is dangerous not only because of its amplitude, it is an exciting factor, which leads to the "manifestation" of signs of other defects in the condition of the equipment. That is why, as part of the diagnostic system built into the drive, there must be a module for monitoring the unbalance of rotating masses.

The presence of other defects shown in Fig. 1 in the diagnostic system will only be ascertained without qualitative and quantitative analysis. Some of the defects are characterized by a catastrophic sudden failure, which is impossible to foresee and arise due to processes or loads of an emergency nature, so there is no point in displaying a failure of this type.

From the analysis of the types of defects and damages in an induction motor, it follows that there are fundamentally different in nature and, accordingly, methods for determining damage groups: one part falls on electrical faults and the second, conditionally, of a mechanical nature. From this it follows that in order to ensure high-quality diagnostics, it is necessary to use blocks with different diagnostic methods in a single block diagram.

Currently, there are a number of disparate methods of non-destructive testing and operational diagnostics that provide a certain degree of reliability of information on individual types of damage. To assess the technical condition of electrical machines, these methods use various diagnostic parameters and, in most cases, to detect the type of malfunction, they require disconnecting the motor from the actuator and taking into account errors in the quality of the supply network. Such systems do not meet modern operating requirements in built-in diagnostic transport systems for work under loading and can be used for bench tests. Currently, the most common following methods of general diagnostics of electric motors are known [20-22]:

- based on the analysis of the electrical properties of the machine;
- control of a condition of insulation;
- based on the analysis of vibrations of individual elements of the unit;
- based on the analysis of acoustic vibrations generated by a working machine;
– based on the measurement and analysis of the magnetic flux in the motor gap and the external magnetic field;
– on the measurement and analysis of the temperature of individual elements of the machine.

In addition, there are a number of defects that must be clarified and repaired when dismantling the electric motor, so the indication of these types is also referred to others, where information about parametric violations of the vibration or electrical type will be received.

Thus, when constructing a block diagram, the most common types of defects in the main elements of an induction electric motor are taken into account, which can be controlled, observed development, predicted uptime and planned repair measures to prevent an emergency stop.

Given the above, the block diagram of the proposed diagnostic system is as shown in Fig. 2.

The diagnostic system built into the drive includes the following modules:

- module for monitoring the occurrence of an inter-turn short circuit;
- module for monitoring the general condition of the insulation;
- module for monitoring the state of the rotor bars;
- module for monitoring the unbalance of the masses of the rotating mechanism;
- module for monitoring the condition of bearings;
- module for monitoring the appearance of other defects.

From the sensor unit, each of the listed modules receives information about the state of the controlled parameters (Fig. 2).

Information about the availability and qualitative and quantitative analysis is displayed on the display unit.

Since the inter-turn short circuit occurs most often during the operation of the engine (Fig. 1) and belongs to a number of difficult-to-diagnose damages, this paper considers a diagnostic system that allows diagnosing this particular defect as part of the drive. The following works of the authors according to the proposed diagnostic structure will be devoted to the issues of diagnosing other defects of an induction motor.

4. DEVELOPMENT OF THE STRUCTURAL DIAGRAM OF THE MODULE FOR MONITORING OF THE APPEARANCE OF INTER-TURN SHORT CIRCUIT

4.1. Rationale for choosing a method for diagnosing an inter-turn short circuit

An inter-turn short circuit in the stator winding phase is the most difficult type of damage to diagnose, which leads to an increase in temperature in closed sections, contributing to the destruction of the insulation and emergency failures of the drive during its long-term operation [23, 24]. It should also be taken into account that the external manifestations caused by this defect are similar in nature to a number of other damages. Therefore, to develop a module for monitoring this defect with determining the degree of damage in industrial conditions of use, it is necessary to decide on the diagnostic method [25, 26].

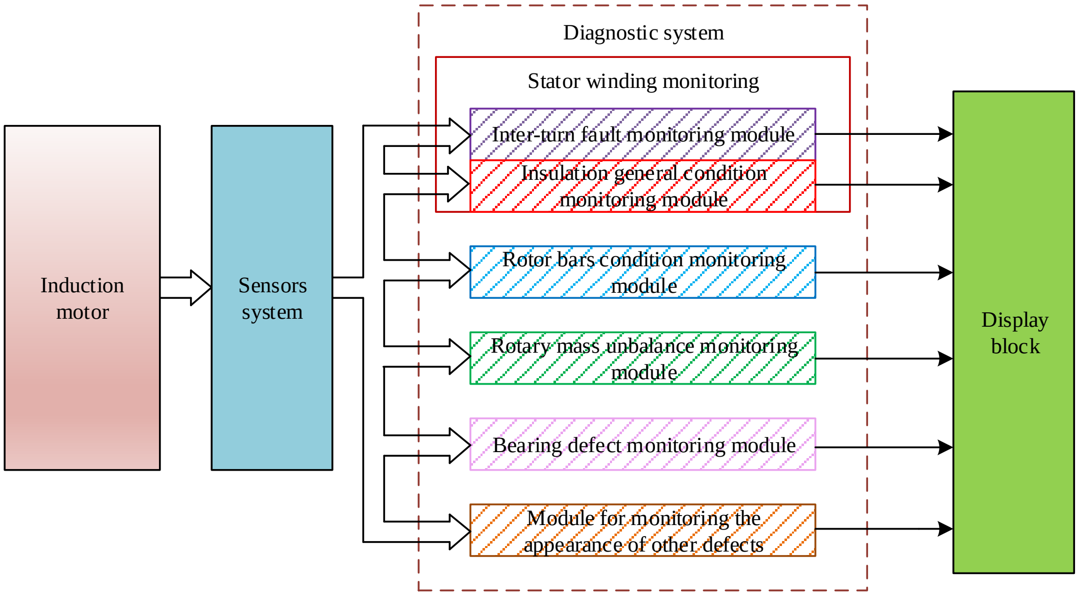

Fig. 2. Block diagram of the proposed diagnostic system

When choosing a diagnostic method, the following reasons should be borne in mind. An induction motor can operate both with a static (for example, motor-fans) and dynamic (for example, a motor-compressor) load [27]. When the load changes, the value of the controlled parameters changes. The quality of the power supply system of the induction motor is an important factor affecting the operation of the diagnostic system. The asymmetry of the power supply voltage system of an induction motor leads to the appearance of torque pulsations, that is, vibrations [28, 29]. The appearance of an inter-turn short circuit has the same signs, since an asymmetric rotating stator field is created. With bench diagnostics, this factor is not important, since the power supply system of the test bench can be made symmetrical.

According to the analysis, the greatest distribution and use in diagnostic systems for the detection, identification and differentiation of faults in the motor can be applied thermal, electrical, vibration and combined diagnostic methods.

The use of thermal methods is considered in [30, 31]. These methods are based on monitoring the thermal state of the stator windings, since with the appearance of an inter-turn short circuit on one of the phases, the average stator current increases and, as a result, the temperature of the windings increases. However, the use of thermal state analysis of thermal state analysis for diagnosing and predicting the failure-free operation time of electric motors is complicated by the current level of development of this method for transport systems.

When using vibration diagnostic methods, the presence and degree of damage in an inductions motor are determined by methods of spectral analysis of vibration signals [13, 14]. Spectra of vibration signals can be used to determine with sufficient accuracy the type and nature of damage, which requires the presence of special sensors. However, a priori data on vibration signals characteristic of different degrees of damage to the stator winding are required to identify the winding defect, its development and predict the run-up time to failure. It was shown in [9] that the coefficient of torque pulsations, which arise as a result of asymmetric modes of the motor windings, is greater at idle than when the motor is operating under load. This factor complicates the application of vibration methods when building a diagnostic system as part of the drive, since the motor in the drive is constantly under load during operation.

The simultaneous appearance of an inter-turn short circuit on two phases is a rather rare case. It is considered in the study [9], where the authors performed a comparison of the coefficient of torque ripples for the case of inter-turn shorting on one and two phases. As a result of the comparison, it was established that with a small number of damaged turns on both phases, the torque ripple coefficient is slightly lower than with the same number of damaged turns on one phase. The coefficient of torque ripples with an increase in the number of damaged turns on two phases gradually becomes greater than the coefficient of torque ripples with the same number of damaged turns on one phase. This indicates the impossibility of using vibration methods to reliably establish the type and degree of the defect.

Diagnostic methods based on the analysis of the distribution of the electromagnetic field of the stator, in particular, on the analysis of the values of the phase currents of the motor stator, are widely used and provide high results in solving a number of complex practical tasks [32, 33].

Therefore, diagnostic methods based on the analysis of stator phase current values should be used in case of unbalanced power supply to establish the type and degree of inter-turn shorting in the stator winding.

4.2. Algorithm for determining the presence of inter-turn short circuit under static load

In [26], in order to detect the presence of stator damage with an asymmetric power system, the main attention is paid to the thermal analysis of an induction motor at the earliest stage of the occurrence of an inter-turn short circuit (two shortened turns). The described methodology does not allow obtaining the degree of closure and is more convenient for bench monitoring of the motor condition. The papers [32, 34] show the effectiveness of applying the Park vector hodograph method related to current diagnostic methods for the same problems.

The essence of the method is as follows. The stator phase currents from the three-phase coordinate system are converted into a moving two-phase coordinate system (dq-coordinates). The hodograph of the Park vector has the form of a regular circle for the case of the absence of asymmetry of the stator windings caused by inter-turn shorting. With a symmetrical system of supply voltages, with the appearance of an inter-turn shorting, the circle transforms into an ellipse. Moreover, with an increase in the number of short-circuited turns, the ellipticity angle ε decreases. In contrast to the case of symmetry of the supply voltage system, in case of asymmetry, the ellipse deviates from the I_{sd} axis by an angle θ (Fig. 3).

Moreover, the deviation by the angle θ in the case of violation of the symmetry of the supply voltage will occur both in the presence and in the absence of damage to the stator windings.

The angle of ellipticity ε will decrease with the appearance of inter-turn short circuits even in the absence of asymmetry of the supply voltage system.

The following designations are adopted in Fig.3:

θ – the orientation angle of the Park vector (the angle between the 0Isd axis and the semi-major axis of the ellipse);

ε – the angle of ellipticity (the angle between the semi-major axis of the ellipse and the diagonal of the rectangle closest to it);

υ - the angle between the semi-major axis of the ellipse and the instantaneous position of the Park vector $\overrightarrow{I_p}$

I_{pmin}, – the value of the Park vector when coinciding with the q axis;

I_{pmax} – the value of the Park vector when it coincides with the d axis;

I_{sd0} – the projection of the Park vector onto the d axis;

I_{sq0} – the projection of the Park vector onto the q axis.

The phase currents of the stator of an induction motor from the three-phase coordinate system are converted to the moving two-phase dq-coordinate system in accordance with the expressions [34]

$$\begin{cases} I_d = I_A \cdot \cos(2\cdot\pi\cdot f\cdot t + \varphi_0) - \\ -\frac{1}{\sqrt{3}}\cdot(I_B - I_C)\cdot\sin(2\cdot\pi\cdot f\cdot t+\varphi_0), \\ I_q = I_A\cdot\sin(2\cdot\pi\cdot f\cdot t+\varphi_0) + \\ +\frac{1}{\sqrt{3}}\cdot(I_B - I_C)\cdot\cos(2\cdot\pi\cdot f\cdot t+\varphi_0), \end{cases} \quad (1)$$

where I_A, I_B, I_C – the values of the phase currents of the induction motor, shown in the ABC coordinates;
f - supply voltage frequency;
φ_0 - the initial phase of the supply voltage of phase A of the motor.

The phase of the space vector of the stator current of an induction motor φ is the angle between the projection of the vector on the rotating two-phase coordinate system and the semi-major axis of the ellipse. The total phase of the space vector of the stator current was determined by the formula [17]

$$\varphi(t) = 2\cdot\pi\cdot f\cdot t + \varphi_0. \quad (2)$$

The total phase of the Park vector to some extent determines the angle υ(t) between the semi-major axis of the ellipse and the instantaneous position of

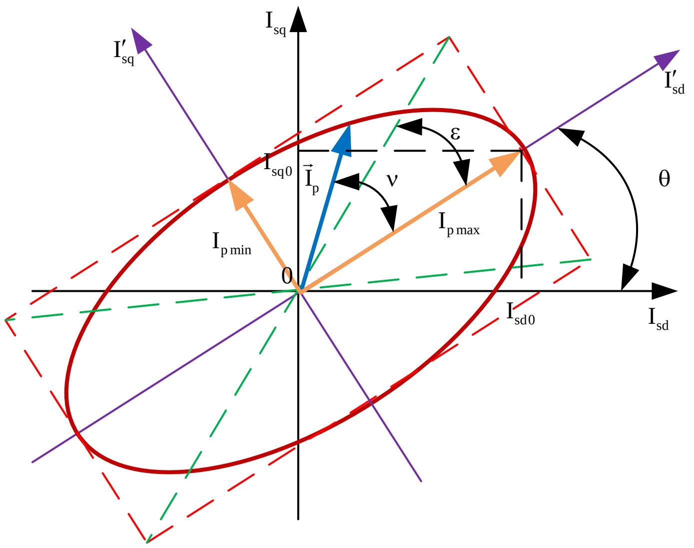

Fig. 3. Hodograph of the Park vector in the presence of damage to the stator winding and asymmetry of the induction motor supply voltage system

the Park vector $\overrightarrow{I_p}$. The angles φ(t) and υ(t) are not equal because the speed of rotation of the Park vector changes during one period. The equality φ = υ occurs when the Park vector $\overrightarrow{I_p}$ coincides with the semi-axes of the ellipse. For other moments of time, the value of the angle υ was determined by the formula [34]

$$\upsilon(t) = \mathrm{arctg}[\mathrm{tg}\varepsilon \cdot \mathrm{tg}\varphi(t)] + \frac{\pi}{2} \cdot \mathrm{sign}\{\sin\varepsilon \cdot \sin\varphi(t)\} \cdot [1 - \mathrm{sign}\{\cos\varepsilon \cdot \cos\varphi(t)\}], \quad (3)$$

where sign[a] means "sign a", i.e. [34]

$$\mathrm{sign[a]} = \begin{cases} 1\ at\ a > 0, \\ -1\ at\ a < 0. \end{cases} \quad (4)$$

In fig. 3 shows the direction of the semi-major axis of the ellipse, the direction of the field vector, and the instantaneous position of the Park vector $\overrightarrow{I_p}$ at the time t=0.

The phase of the spatial current vector is determined using these parameters. The angle between the Park vector $\overrightarrow{I_p}$ and the semi-major axis of the ellipse will determine the phase φ of the space vector of the stator phase current. Positive values of the angle φ will be those placed in the direction of rotation of the field. The angle υ is the phase of the Park vector, and the angle φ is the angle of the space vector of the stator phase current.

The studies were carried out using a simulation model of an induction motor, executed in the MATLab software environment [35] with the established level of accuracy of the results obtained [36]. When conducting research, the factor was taken into account that during transient processes in an induction motor, the amplitudes of phase currents change. This entails a change in the shape of the Park vector hodograph. For this purpose, studies were carried out for the steady state operation of the electric motor.

When conducting research, the hypothesis that the supply voltage system is symmetrical is first accepted, and the obtained results of the stator phase currents are processed in an orthogonal-circular basis.

The angle of ellipticity for an orthogonal-circular basis is equal to [34]

$$\varepsilon = \mathrm{arctg}\frac{I_{pmin}}{I_{pmax}}. \quad (5)$$

For an orthogonal-circular basis, the relations $I_{pmax} = I_{pmin} = I_{sd0}$ are valid. That is, with the symmetry of the induction motor windings and the stator voltage system, the hodograph of the Park vector describes a circle, which is a local case of an ellipse. For this case, the statement that the angles of ellipticity of orthogonal-circular and orthogonal-elliptic bases are equal is correct, that is, ε=γ.

After that, the hypothesis about the symmetry of the supply voltage systems should be tested. A sign of the asymmetry of the supply voltage systems is the non-zero value of the ellipse slope angle (see Fig. 3). Calculations of the angle of ellipticity and the angle of inclination of the ellipse in this case should be made in an orthogonal-elliptical basis.

The angle of ellipticity in the orthogonal-elliptic basis is equal [34]

$$\gamma = \mathrm{arctg}\frac{I_{sq0}}{I_{sd0}}. \quad (6)$$

The angle of inclination of the ellipse is equal [34]

$$\theta = \arccos\frac{I_{sd}}{I_{pmax}} = \arcsin\frac{I_{sq}}{I_{pmax}}. \quad (7)$$

After that, it is necessary to enumerate the values of the projections of the Park vector obtained in the orthogonal-circular basis to the orthogonal-elliptic one. Enumerations are made in accordance with the expressions [34]

$$\begin{gathered} i'_{sd0} = (\cos\varepsilon_0 \cdot \cos\theta_0 - j \cdot \sin\varepsilon_0 \cdot \sin\theta_0) \cdot I_{sd0} \\ +j(\cos\varepsilon_0 \cdot \sin\theta_0 + j \cdot \sin\varepsilon_0 \cdot \cos\theta_0) \cdot I_{sq0}; \\ i'_{sq0} = \left(\cos(-\varepsilon_0) \cdot \cos\left(\theta_0 + \frac{\pi}{2}\right) - \right. \\ \left. -j \cdot \sin(-\varepsilon_0) \cdot \sin\left(\theta_0 + \frac{\pi}{2}\right)\right) + \\ +j\left(\cos(-\varepsilon_0) \cdot \sin\left(\theta_0 + \frac{\pi}{2}\right) + \right. \\ \left. +j \cdot \sin(-\varepsilon_0) \cdot \cos\left(\theta_0 + \frac{\pi}{2}\right)\right) \cdot I_{sq0}, \end{gathered} \quad (8)$$

where ε_0 – the angle of ellipticity of the basic unit vector relative to the d axis in the new basis. Relative to the q axis, the value of the angle $\varepsilon_0=0$. In the orthogonal-circular basis $\varepsilon_0=\pi/4$;
θ_0 - the angle of inclination of the basic basis vector ellipse relative to the d axis in the new basis. Relative to the q axis, the value of this angle is $\theta_0=\pi/2$. In the orthogonal-circular basis relative to the d axis, $\theta_0=0$.

The amplitude values of the currents i'_{sd0} and i'_{sq0} are calculated by the formulas [34]

$$\begin{cases} I'_{sd0} = \sqrt{\left(\mathrm{Re}(i'_{sd0})\right)^2 + \left(\mathrm{Im}(i'_{sd0})\right)^2}, \\ I'_{sq0} = \sqrt{\left(\mathrm{Re}(i'_{sq0})\right)^2 + \left(\mathrm{Im}(i'_{sq0})\right)^2}. \end{cases} \quad (9)$$

The value of the angle of ellipticity in the new basis was calculated according to formula (5). The values of I'_{sd0} and I'_{sq0}, calculated according to the formulas (10), were substituted into the formula (5) instead of the values of I_{sd0} and I_{sq0}, respectively.

The presence of an inter-turn short circuit in the will be indicated by the ellipticity angle ε, the value of which will be less than π/4.

The method of determining the number of damaged turns due to inter-turn shorting in the stator windings of an electric motor is given in the study [34]. Dependences of deviations of amplitudes and displacements of phase shift angles of stator currents, as functions of the number of damaged turns of stator windings, are linear, it was noted in this study.

The difference between the values of the amplitude of the stator phase current of the controlled phase in the presence and absence of inter-turn shorting is the deviation of the amplitude of the stator phase current.

The difference between the values of the angle of the stator phase current and the stator voltage of the controlled phase in the presence and absence of inter-turn shorting is the displacement of the phase shift angles of the stator currents. The number of damaged turns can be determined with absolute accuracy in the presence of experimental values of the deviation of the amplitudes of the phase currents and the displacement of the phase shift angles of the stator currents for the motor under consideration at any moment of its operation.

For this purpose, the slope of the increase in the stator current is calculated [34]

$$k_{Is} = \frac{I_s - I_{snom}}{n}. \quad (10)$$

and the displacement coefficient of the phase shift angle of the stator current [34]

$$k_{\varphi Is} = \frac{\varphi_{Is} - \varphi_{Isnom}}{n}. \quad (11)$$

In formulas (10) and (11):

I_s – the instantaneous value of the stator current of the monitored phase;

I_{snom} – the instantaneous value of the stator ~~phase~~ current in the absence of an inter-turn short circuit;

n – the number of damaged turns;

φ_{Is} – the value of the phase shift angle of the stator current of the monitored phase;

φ_{Isnom} - nominal value of the stator current phase displacement angle.

Coefficients (11) and (12) are calculated for the same regime both in the absence and presence of damage to the stator winding.

The number of damaged turns was calculated for each phase based on the obtained amplitudes and phase shift angles of the stator currents in the presence of the values of the coefficients using the formulas [34]

$$n = \frac{I_s - I_{snom}}{k_{Is}}. \quad (12)$$

$$n = \frac{\varphi_{Is} - \varphi_{Isnom}}{k_{\varphi Is}}. \quad (13)$$

The amplitudes and phases of the stator ~~phase~~ currents are determined by the formulas [34]

$$\begin{cases} \varphi_{IsAm} = \mathrm{arctg}(\mathrm{tg}\gamma \cdot \mathrm{tg}\varphi_{snom}), \\ \varphi_{IsBm} = \mathrm{arctg}\left(\mathrm{tg}\gamma \cdot \mathrm{tg}\left(\varphi_{snom} - \frac{2\cdot\pi}{3}\right)\right), \\ \varphi_{IsCm} = \mathrm{arctg}\left(\mathrm{tg}\gamma \cdot \mathrm{tg}\left(\varphi_{snom} + \frac{2\cdot\pi}{3}\right)\right). \end{cases} \quad (14)$$

$$\begin{cases} I_{sAm} = ((I'_{sd0} \cdot \cos(\Delta\varphi_{sIAm}))^2 + \\ \quad + \left(I'_{sq0} \cdot \sin(\Delta\varphi_{sIAm})\right)^2\Big)^{-\frac{1}{2}}, \\ I_{sBm} = \left(\left(I'_{sd0} \cdot \cos\left(\Delta\varphi_{sIAm} - \frac{2\cdot\pi}{3}\right)\right)^2 + \right. \\ \quad \left. + \left(I'_{sq0} \cdot \sin\left(\Delta\varphi_{sIAm} - \frac{2\cdot\pi}{3}\right)\right)^2\right)^{-\frac{1}{2}}, \\ I_{sCm} = \left(\left(I'_{sd0} \cdot \cos\left(\Delta\varphi_{sIAm} + \frac{2\cdot\pi}{3}\right)\right)^2 + \right. \\ \quad \left. + \left(I'_{sq0} \cdot \sin\left(\Delta\varphi_{sIAm} + \frac{2\cdot\pi}{3}\right)\right)^2\right)^{-\frac{1}{2}}. \end{cases} \quad (15)$$

In formula (14), φ_{snom} is the value of the phase shift angle of the stator currents with intact ~~stator~~ windings.

The results are rounded up to an integer. The largest integer is selected among the results obtained, which will correspond to the number of damaged windings. The damaged phase is selected based on the largest value of the modulus of the stator current increase coefficient and the largest value of the phase shift angle displacement coefficient [34].

4.3. Algorithm for determining the presence of inter-turn short circuit under dynamic load

The method that allows diagnosing the presence of an inter-turn short circuit in the stator windings of an induction motor in dynamic mode in the presence of a defect both on one phase and on two at the same time is given in the study [9]. Options for modeling dynamic loads in combined transport trains are also considered in [27].

If an inter-turn short circuit is present in the stator windings, then when the motor shaft rotation frequency changes (that is, when the motor load changes), the changes in phase shifts Δφ between the phase currents and voltages for each phase will be the same, it was noted in the study [9], i.e.

$$\Delta\varphi_{Ai} = \Delta\varphi_{Bi} = \Delta\varphi_{Ci} = \Delta\varphi_i, \quad (16)$$

where $\Delta\varphi_i$ – the phase shift between phase current and voltage for the i-th motor rotor speed

$$\Delta\varphi_i = \varphi_i - \varphi_{i-1}, \quad (17)$$

where φ_i – the phase shift between phase currents and voltages at the motor shaft speed n_i;

φ_{i-1} – phase shift between phase currents and voltages at motor shaft speed n_{i-1}.

Based on formula (16), the additional diagnostic parameter χi is introduced to estimate the change in the phase shift between phase currents and voltages when the motor shaft rotation frequency increases [9]

$$\chi_i = \frac{\Delta\varphi_i}{\Delta n_i}, \quad (18)$$

where Δn_i

$$\Delta n_i = n_i - n_{i-1}. \quad (19)$$

The parameters of the rate of change of the increment of the phase shift between the phase currents and voltages when changing the frequency of rotation of the motor shaft (induction motor of the AIR 132M4 series with a power of 11.0 kW) are shown in Fig. 4. The degree of damage to the stator (the number of closed turns) is taken into account by reducing the nominal total resistance of the winding [9]:

- with intact (serviceable) stator (χ);
- at 90% of undamaged winding turns of one phase (χ_1);
- at 80% of undamaged winding turns of one phase (χ_2);

- at 80% undamaged winding turns of one phase and 90% undamaged winding turns of the second phase simultaneously (χ_3);
- at 80% undamaged winding turns of one phase and 80% undamaged winding turns of the second phase simultaneously (χ_4).

Dependencies shown in Fig. 4, have a jump-like character in the region of the idling mode and engine shaft rotation frequencies close to it (range 1498-1488 rpm). This range shaft rotation frequency corresponds to a low motor load and cannot be used for diagnostic purposes. As the motor load increases, there are long linear sections that continue almost to the nominal engine shaft speed (Fig. 4). So, for undamaged stator windings, the range of the linear section is from 1490.8 rpm to 1450 rpm, when one phase is damaged, from 1485.8 rpm to 1458.32 rpm, when two phases are damaged, from 1485.8 rpm to 1466.4 rpm.

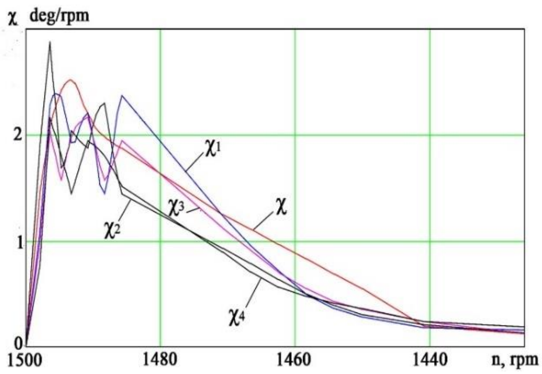

Fig. 4. Dependence of the rate of change of the phase shift (χi, deg/rpm) on the frequency of rotation of the motor shaft (n, rpm)

It follows that the range of the linear section of the dependence χ=f(n) decreases with an increase in the number of damaged stator phases. As a result of the analysis of the dependencies shown in Fig. 4, the following conclusion is made. The second derivative of the change in phase shift according to the frequency of rotation of the motor shaft when the same number of phases is damaged at different degrees of damage changes differently [9]

$$\xi_i = \frac{\chi_i}{\Delta n_i}. \quad (20)$$

The parameter ξ from expression (20) can be used as a criterion in the construction of a diagnostic system for the diagnosis of induction motor defects caused by inter-turn short circuits of the stator windings.

4.4. Development of a block diagram of the module for monitoring the presence of an inter-turn short circuit under static and dynamic loads of the electric motor

Based on the algorithms developed above for diagnosing the presence of an inter-turn short circuit under static and dynamic loads of an induction electric motor, a block diagram of the module for monitoring the presence of an inter-turn short circuit has been developed (Fig. 5).

To select an algorithm for monitoring the occurrence of a short circuit, it is necessary to determine at what load the induction motor operates - with a static or dynamic load. For this purpose, an angular velocity sensor is used. In the "Comparison block of the current and previous values of the angular velocity" the parameter is determined

$$\Delta\omega = \omega_i - \omega_{i-1}, \quad (22)$$

where ω_i – the current value of the angular velocity; ω_{i-1} – the previous value of the angular velocity.

When $\Delta\omega$=0, the "Control mode selection" block turns on the control channel under static load, at $\Delta\omega\neq 0$ - the control channel under dynamic load.

Since the current method was chosen to diagnose the occurrence of an inter-turn short circuit, current sensors are used to obtain the value of phase currents. In this case, one should keep in mind the fact that an induction electric motor can be powered by an autonomous voltage inverter, therefore, the supply voltage system can be non-sinusoidal. Therefore, to determine the amplitude and phase of the first (fundamental) harmonic of the stator phase currents (I_{sA1}, I_{sB1}, I_{sC1}, φ_{IsA1}, φ_{IsB1}, φ_{IsC1}), the Fast Fourier Transform Block is used. The "Fast Fourier Transform Block" is also needed to determine the phases of the first harmonics of the stator phase voltages (φ_{UsA1}, φ_{UsB1}, φ_{UsC1}). The phases of the first harmonics of the phase voltages and stator currents are necessary to determine the phase displacements between the phase voltages and stator currents.

The amplitudes of the first harmonics of the stator phase currents (I_{sA1}, I_{sB1}, I_{sC1}) and the frequency of the first harmonic of the stator phase voltages (f_1) enter the "Block of coordinate transformations", where the phase currents are converted from a three-phase coordinate system into a two-phase moving dq coordinate system in accordance with the expressions (15).

the obtained values of the phase currents in the dq coordinate system are sent to the "Block for calculating the parameters of the Park vector hodograph", where the projections of the Park vector hodograph on the d axis (I_{sd0}), on the q axis (I_{sq0}) and the angle of ellipticity in the orthogonal-elliptical basis (γ) (7). "Block of coordinate transformations" is switched on when it receives a signal from the "Select control mode" block.

The obtained values of I_{sd0}, I_{sq0} and γ are sent to the "Block of transition from orthogonal-elliptic basis to orthogonal-circular and determination of the presence of inter-turn closure", in which, based on expressions (9), (10), the values of the projections of the Park vector hodograph from the orthogonal-elliptic basis to orthogonally circular. After that, according to expression (7), the coefficient of ellipticity is calculated in the new basis. The obtained value of the angle of ellipticity less than $\pi/4$ will indicate the presence of an inter-turn short circuit in the stator windings.

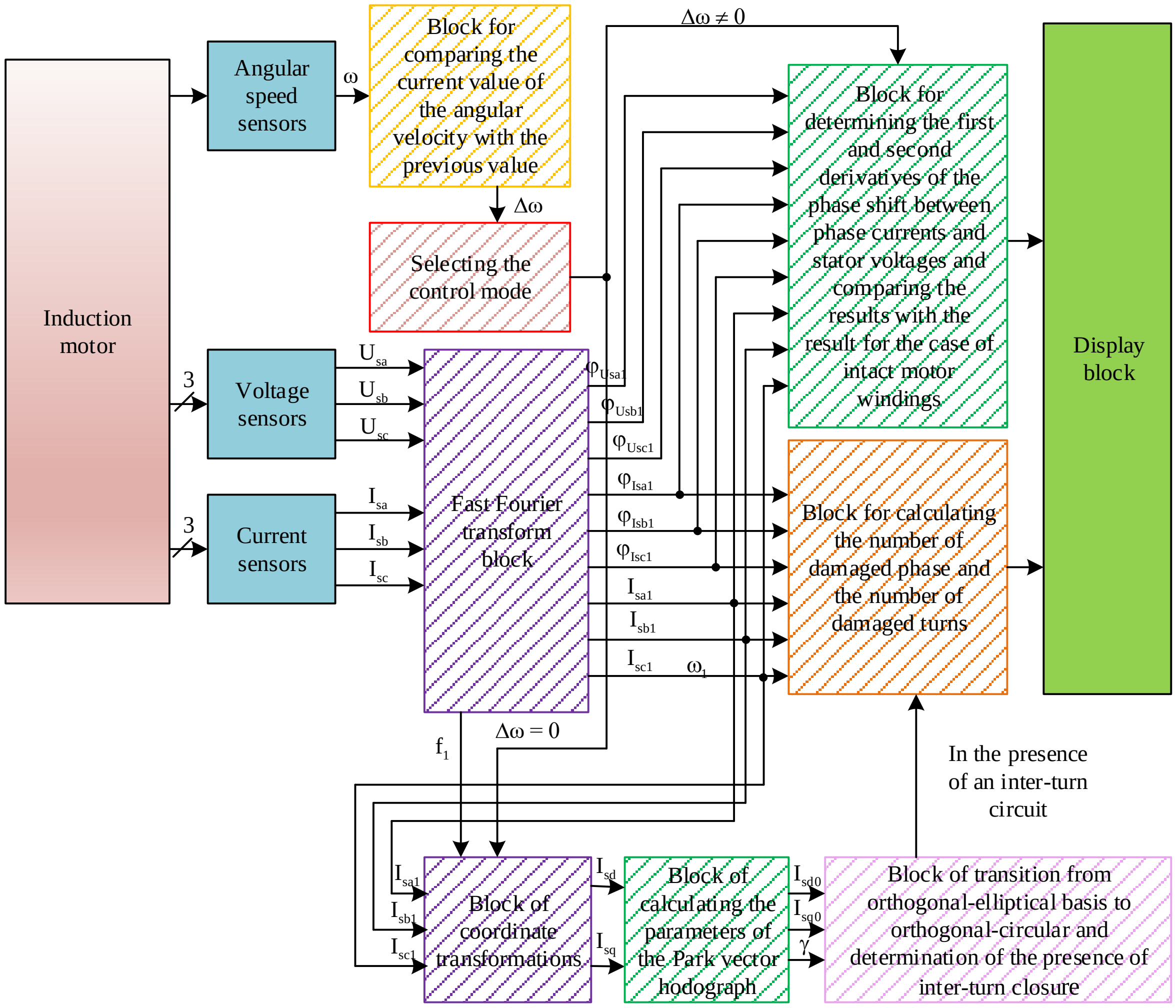

Fig. 5. Structural diagram of the module for monitoring the occurrence of an inter-turn short circuit

In the presence of an inter-turn short circuit, the amplitudes and phases of the stator phase currents are calculated using expressions (15-16), and the number of damaged turns of the winding stator is calculated using expressions (13-14).

The results of monitoring the occurrence of an inter-turn short circuit under static load are displayed ("Display block").

With a signal from the output of the "Control mode selection" block, which includes a channel for determining the presence of an inter-turn short circuit under dynamic load, the amplitudes of the phase currents, the amplitudes and phases of the first harmonic of the stator phase currents and the phase of the first harmonics of the stator phase voltages from the "Fast Fourier transform block" are sent to " Block for determining the first and second derivatives of the phase shift between phase currents and stator voltages and comparing the result with the result for the case of undamaged motor windings, where the first and second derivatives of the phase shift between phase currents and stator voltages are calculated in accordance with expressions (20) and (21) respectively. Comparison of the obtained and experimental results of the second derivative of the phase shift between the phase currents and stator voltages makes it possible to determine the number of damaged phases and the number of damaged turns in each phase.

The results of monitoring the occurrence of an inter-turn short circuit under dynamic load are displayed ("Display block").

Thus, the developed module for monitoring the presence of inter-turn short circuits in one or more phases of the winding stator allows to determine the damaged phase and the number of closed turns under static and dynamic loads of the electric motor, regardless of the quality of the supply voltage. Setting the degree of damage to the stator winding of the electric motor by the number of closed turns allows to predict the time of trouble-free operation and plan the repair of transport equipment.

4. CONCLUSION

This work is completed in a set of studies on the study of the manifestation and influence of inter-turn short circuits in the stator winding of an induction motor and the construction of a module for determining the type and degree of this type of damage for use in the system of technical control of the state of vehicle electric motors.

As a result of the analysis of damages and methods for diagnosing induction electric motors, a block diagram of the built-in diagnostic system has been developed.

The diagnostic system built into the drive includes the following modules:

- control of occurrence of inter-turn short circuit;
- control of the general condition of the insulation;
- monitoring the condition of the rotor bars;
- control of unbalance of masses of the rotating mechanism;
- monitoring the condition of bearings;
– control of the appearance of other defects.

To create a diagnostic system module for determining and differentiating the type and degree of inter-turn short circuit in the stator phase winding, the most difficult to diagnose damage, studies using mathematical modeling were used.

Studies to determine the degree of damage to the motor stator winding with an asymmetric supply voltage system and a static load have shown the effectiveness of using the Park vector hodograph method. According to the proposed method, the number of damaged turns in the presence of an inter-turn short circuit in the stator windings of an electric motor depends on the deviations of the amplitudes of the stator phase currents and the shifts in the phase shift angles of the stator currents and is linear.

Calculation of the amplitudes and angles of the phase displacement of stator currents for each phase makes it possible to determine the number of damaged turns with a high accuracy of determining the presence of an inter-turn short circuit under a static load with a possible asymmetric supply voltage.

The conducted studies of the influence of the degree of inter-turn short circuit on phase shifts between phase voltages and currents when the motor load changes showed that phase shifts remain the same for all phases of the motor when the shaft speed changes throughout the entire operating range of the motor - from 1425.7 rpm to 1498.0 rpm . An analysis of the obtained dependences of the influence of the degree of inter-turn short circuit on phase shifts between phase voltages and currents with a change in the motor load showed that the dependences χ=f(n) have ranges with linear sections, and with an increase in the number of damaged phases, the range of the linear section of the characteristics decreases. For damage to one stator phase - from 1485.8 rpm to 1458.32 rpm; for damage to two phases of the stator - from 1485.8 rpm to 1466.4 rpm, etc. Reducing the range of the straight section χ=f(n) with an increase in the number of damaged phases and the degree of damage (the number of closed turns) is used in the construction of a block for the presence of an inter-turn short circuit under dynamic load in the module of the stator winding condition monitoring system.

On the basis of the research, an algorithm has been developed and a block diagram of the module for monitoring the presence of an inter-turn short circuit under static and dynamic load of the electric motor has been developed for operation as part of the built-in diagnostic system for transport equipment. The developed block diagram is ready for subsequent implementation in physical form and use in operating conditions.

Author contributions: *research concept and design, O.G.; Collection and/or assembly of data, S.D., M.Y.; Data analysis and interpretation, O.G., S.D., I.M.; Writing the article, S.D., I.M., M.Y.; Critical revision of the article, O.G.; Final approval of the article, O.G.*

Declaration of competing interest: *The authors declare that they have no known competing financial interests or personal relationships that could have appeared to influence the work reported in this paper.*

REFERENCES

1. Sheikh MA, Bakhsh ST, Irfan M, Nor NBM, Nowakowski G. A Review to Diagnose Faults Related to Three-Phase Industrial Induction Motors. J Fail. Anal. And Preven. 2022:1-12. https://doi.org/10.1007/s11668-022-01445-2.
2. Hussein AM, Obed AA, Zubo RA, Al-Yasir YI, Saleh AL, Fadhel H, Sheikh-Akbari A, Mokryani G, Abd-Alhameed RA. Detection and Diagnosis of Stator and Rotor Electrical Faults for Three-Phase Induction Motor via Wavelet Energy Approach. Electronics. 2022;11(8):1253. https://doi.org/10.3390/electronics11081253.
3. Choudhary A, Goyal D, Shimi SL, Akula A. Condition monitoring and fault diagnosis of induction motors: A review. Archives of Computational Methods in Engineering. 2019;26(4):1221-1238. https://doi.org/10.1007/s11831-018-9286-z.
4. Regaz A, Zegnini B, Djellali M, Boukezzi L. Detection of faults in the induction machine by the use of smart materials. Diagnostyka. 2018;19(3):43-54. https://doi.org/10.29354/diag/93230.
5. Abdelhak G, Sid Ahmed B, Djekidel R. Fault diagnosis of induction motors rotor using current signature with different signal processing techniques. Diagnostyka. 2022;23(2): 2022201. https://doi.org/10.29354/diag/147462.
6. Bazan GH, Goedtel A, Duque-Perez O, Morinigo-Sotelo D. Multi-fault diagnosis in three-phase induction motors using data optimization and machine learning techniques. Electronics, 2021;10:1462. https://doi.org/10.3390/electronics10121462.
7. Dehina W, Boumehraz M. Experimental investigation in induction motors using signal processing techniques for early detection of inter-turn short circuit faults. International Journal of Modelling and Simulation, 2021:855-867. https://doi.org/10.1080/02286203.2021.2001635.
8. Gubarevych O, Goolak S, Daki O, Tryshyn V. Investigation of turn-to-turn closures of stator windings to improve the diagnostics system for induction motors. Problemele energeticii regionale. 2021;2(50):10–24. https://doi.org/10.52254/1857-0070.2021.2-50.02.
9. Gubarevych O, Goolak S, Daki O, Yakusevych Y. Determining an additional diagnostic parameter for improving the accuracy of assessment of the condition

of stator windings in an induction motor. Eastern-European Journal of Enterprise Technologies, 2021; 5(113):21–29. https://doi.org/10.15587/1729-4061.2021.239509.
10. Haiba1 AS, ElFaraskoury AA, ElKoshairy AD, Halawa MM. Modeling and simulation of partial discharge measurement for defected solid dielectrics. Journal of Measurement Science and Applications (JMSA). 2022;2(1):43-53. https://doi.org/10.21608/JMSA.2022.219865.
11. Tsyokhla A, Griffo I, Wang J. On-line motor insulation capacitance monitoring using low-cost sensors. 2019 IEEE Energy Conversion Congress and Exposition (ECCE), 2019:6996-7003. https://doi.org/10.1109/ECCE.2019.8912241.
12. Kuncan M, Kaplan K, Minaz MR, Kaya Y, Ertunc H M. A novel feature extraction method for bearing fault classification with one dimensional ternary patterns. ISA transactions. 2020;100:346-357. https://doi.org/10.1016/j.isatra.2019.11.006.
13. Pusca R, Sbaa S, Bessous N, Romary R, Bousseksou R. Mechanical failure detection in induction motors using stator current and stray flux analysis techniques. Eng. Proc. 2022;14:19. https://doi.org/10.3390/engproc2022014019.
14. Safiullin RA. Vibration diagnostics of induction motors. 2021 International Conference on Electrotechnical Complexes and Systems (ICOECS), 2021:228-232. https://doi.org/10.1109/icoecs52783.2021.9657352.
15. Benbouzid MEH. Signal processing for fault detection and diagnosis in electric machines and systems. IET, London. 2020:284. https://doi.org/10.1049/PBPO153E_itr.
16. Asad B, Vaimann T, Belahcen A, Kallaste A. Broken rotor bar fault diagnostic of inverter fed induction motor using FFT, Hilbert and Park's vector approach. In 2018 XIII International Conference on Electrical Machines (ICEM). IEEE, 2018:2352-2358. https://doi.org/10.1109/ICELMACH.2018.8506957.
17. Goktas T. Evaluation and Classification of Double Bar Breakages Through Three-Axes Vibration Sensor in Induction Motors. In IEEE Sensors Journal, 1 July1, 2022;22(13):13602-13611. https://doi.org/10.1109/JSEN.2022.3176059.
18. Sabir H, Ouassaid M, Ngote N, Benbouzid M. A novel experimental method to detect early rotor faults in induction machines. International Journal on Energy Conversion (IRECON). 2021;9(5):191-202. https://doi.org/10.15866/irecon.v9i5.21214.
19. Suechoey B, Siripornanon S, Chupun P, Boonkhun C, Chompooinwai C. Performance analysis and fault classification in a large electric motor using vibration assessment technique. International Journal of Intelligent Engineering and Systems. 2021;14(1): 124–133. https://doi.org/10.22266/ijies2021.0228.13.
20. Almounajjed A, Sahoo AK, Kumar MK, Assaf T. Fault diagnosis and investigation techniques for induction motor. International Journal of Ambient Energy. 2022:1-21. https://doi.org/10.1080/01430750.2021.2016483
21. Muxiri AC, Bento F, Fonseca DSB, Cardoso AJM. Thermal analysis of an induction motor subjected to inter-turn short-circuit failures in the stator windings. In 2019 International Conference on Industrial Engineering, Applications and Manufacturing (ICIEAM). 2019:1-5. https://doi.org/10.1109/ICIEAM.2019.8743076.
22. Varbanets R, Fomin O, Píštěk V, Klymenko V, Minchev D, Khrulev A, Zalozh V, Kučera P. Acoustic method for estimation of marine low-speed motor turbocharger parameters. Journal of Marine Science and Engineering. 2021;9(3):321. https://www.mdpi.com/2077-1312/9/3/321/htm.
23. Asfani DA, Negara IMY, Hernanda IGNS, Fahmi D, Muljadi E, Nelms RM. Methods to Deter006Dine the Stator Inter-turn Short Circuit in an Induction Motor with Installed Rotor. In: 2020 IEEE Energy Conversion Congress and Exposition (ECCE). 2020: 7-13. https://doi.org/10.1109/ECCE44975.2020.9236051.
24. Hegde V, Sathyanarayana Rao MG. Detection of stator winding inter-turn short circuit fault in induction motor using vibration signals by MEMS accelerometer. Electric Power Components and Systems. 2017;45(13):1463-1473. https://doi.org/10.1080/15325008.2017.1358777.
25. Singh G, Kumar TCA, Naikan VNA. Induction motor inter turn fault detection using infrared thermographic analysis. Infrared Physics & Technology. 2016;77: 277-282. https://doi.org/10.1016/j.infrared.2016.06.010.
26. Adouni A, J Marques Cardoso A. Thermal analysis of low-power three-phase induction motors operating under voltage unbalance and inter-turn short circuit faults. Machines. 2021;9(1):2-11. https://doi.org/10.3390/machines9010002.
27. Lovska A, Fomin O, Pistek V, Kucera P. Dynamic load modelling within combined transport trains during transportation on a railway ferry. Applied Sciences. 2020;10(16):5710. https://www.mdpi.com/2076-3417/10/16/5710.
28. Goolak S, Gubarevych O, Gorobchenko O, Nevedrov O, Kamchatna-Stepanova K. Investigation of the influence of the quality of the power supply system on the characteristics of an induction motor with a squirrel-cage rotor. Przegląd Elektrotechniczny, 2022; 98(6(1)):142–148. https://doi.org/10.15199/48.2022.06.26.
29. Goolak S, Tkachenko V, Šťastniak P, Sapronova S, Liubarskyi B. Analysis of control methods for the traction drive of an alternating current electric locomotive. Symmetry. 2022;14(1):150. https://doi.org/10.3390/sym14010150.
30. Muxiri AC, Bento F, Fonseca DSB, Cardoso AJM. Thermal analysis of an induction motor subjected to inter-turn short-circuit failures in the stator windings. In 2019 International Conference on Industrial Engineering, Applications and Manufacturing (ICIEAM). IEEE. 2019:1-5. https://doi.org/10.1109/ICIEAM.2019.8743076.
31. Singh G, Kumar TCA, Naikan VNA. Induction motor inter turn fault detection using infrared thermographic analysis. Infrared Physics & Technology. 2016;77: 277-282. https://doi.org/10.1016/j.infrared.2016.06.010.
32. Sha M, Luo M. Online identification technology based on variation mechanism of traction motor parameters. In 2021 4th International Conference on Advanced Electronic Materials, Computers and Software Engineering (AEMCSE). IEEE. 2021:77-82. https://doi.org/10.1109/AEMCSE51986.2021.00023.
33. Benbouzid MEH. A review of induction motors signature analysis as a medium for faults detection, IEEE Transactions on Industrial Electronics, 2000; 47(5): 984-993. https://doi.org/10.1109/41.873206.

34. Gerlici J, Goolak S, Gubarevych O, Kravchenko K, Kamchatna-Stepanova K, Toropov A. Method for determining the degree of damage to the stator windings of an induction electric motor with an asymmetric power system. Symmetry. 2022;14:1305. https://doi.org/10.3390/sym14071305.
35. Goolak S, Gerlici J, Gubarevych O, Lack T, Pustovetov M. Imitation modeling of an inter-turn short circuit of an induction motor stator winding for diagnostics of auxiliary electric drives of transport infrastructure. Communications-Scientific letters of the University of Zilina. 2021;23(2):C65–C74. https://doi.org/10.26552/com.C.2021.2.C65-C74.
36. Gubarevych O, Golubieva S, Melkonova I. Comparison of the results of simulation modeling of an induction electric motor with the calculated electrodynamic and energy characteristics. Przegląd Elektrotechniczny. 2022;98(10):61-66. https://doi.org/10.15199/48.2022.10.11.

Received 2022-10-06
Accepted 2022-11-08
Available online 2022-11-09

Oleg GUBAREVYCH
PhD, Associate Professor Corresponding Member of the Academy of Applied Sciences Department of Electromechanics and Rolling Stock of Railways of State University of Infrastructure and Technologies, Kyiv, Ukraine.
His main research focused on improving reliability and methods for diagnosing electrical equipment.
E-mail: oleg.gbr@ukr.net

Sergey GOOLAK
PhD, Associate Professor
Department of Electromechanics and Rolling Stock of Railways of State University of Infrastructure and Technologies, Kyiv, Ukraine. Scientific interests – technical diagnostics of drives of transport systems.
E-mail: sgoolak@gmail.com

Inna MELKONOVA
PhD, Associate Professor
Department of Electrical Engineering of Volodymyr Dahl East Ukrainian National University, Ukraine.
Scientific interests – magnetic separation, renewable energy, electric drive.
E-mail: inna.mia.lg@gmail.com

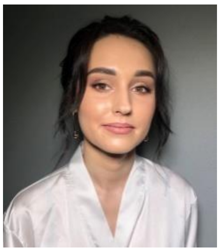

Mariia YURCHENKO
Postgraduate student.
Faculty of Management and Technology of State University of Infrastructure and Technologies, Kyiv, Ukraine.
Scientific interests - Optimization of the work of shipbuilding and ship repair plants.
E-mail: mlysenkova27@gmail.com